

Short Papers

Niobium Microbolometers for Far-Infrared Detection

Michael E. MacDonald and Erich N. Grossman

Abstract—Microbolometers have been fabricated using a thin niobium film as the detector element. These detectors operate at room temperature, are impedance matched to planar antennas, and are suitable for broadband use at far-infrared wavelengths. We have achieved responsivities of up to 21 V/W at a bias of 6.4 mA, and electrical noise equivalent powers (NEP) of as low as 1.1×10^{-10} W/ $\sqrt{\text{Hz}}$ at 1 kHz at a bias of 3.6 mA. At this bias, the detectors are $1/f$ -noise limited below 1 kHz and are Johnson noise limited above 10 kHz. The $1/f$ noise in nV/ $\sqrt{\text{Hz}}$ increases approximately linearly with bias with a typical level of $0.39 \frac{I(\text{mA})}{\sqrt{f(\text{kHz})}}$. This level of $1/f$ noise is approximately a factor of 7 below the best reported for bismuth microbolometers.

I. INTRODUCTION

Bolometric detectors are advantageous at far-infrared wavelengths (10–1000 μm) because they possess an inherently flat frequency response. Any bolometer has two functional components which must be thermally coupled to one another: an absorber which converts incident radiation into heat, and a thermometer which monitors the resulting temperature change. These can be physically distinct from each other, as in the micromachined Golay cell [1], or they may be combined in the same physical component as in the large-area bismuth radiometer [2]. In a conventional bolometer, the surface of the absorber must be at least one square wavelength in area in order to receive radiation efficiently. This imposes a major limitation on the device's speed, since a large area implies a large thermal mass. This limitation is overcome by coupling radiation through a planar antenna into an absorber element which is much less than a wavelength in size. In such “microbolometers” [3] the detector element is made as small as is practical, in order to obtain fast response and high responsivity. The detector must be illuminated through the substrate in order to achieve high efficiency [4].

Several construction methods have been employed for microbolometer detectors. One type, similar to the present case, employs a thin bismuth film as both an absorber and a resistive thermometer [5]. Bismuth-antimony thermocouples have been fabricated and have the advantage that no biasing is required, so that there is no $1/f$ noise [6]. In this work, we describe the use of a 20–30 nm thick niobium film as both absorber and thermometer. The niobium microbolometer is found to have much lower $1/f$ noise than comparable bismuth devices. This implies that noise-equivalent powers are obtained with a niobium device deposited directly on a substrate that are similar to those of a bismuth device fabricated as a free-standing “airbridge” [7]. These niobium microbolometers can be manufactured much more easily, inexpensively and reproducibly than bismuth airbridge detectors.

Manuscript received November 12, 1993; revised July 19, 1994. This work was supported in part by the Office of Innovative Science and Technology, through ONR, and by the Astrophysics Division of NASA.

The authors are with the National Institute of Standards and Technology, Boulder, CO 80303 USA.

IEEE Log Number 9408582..

II. DEVICE DESIGN AND FABRICATION

The antenna we have used is an equiangular spiral, with a 65° wrap angle and 90° arm width resulting in a self-complementary design [8]. The antenna impedance is purely real and is given by

$$Z_a = \frac{Z_0}{\sqrt{2(1 + \varepsilon_r)}}, \quad (1)$$

where $Z_0 = 377 \Omega$ is the intrinsic impedance of free space, and ε_r is the dielectric constant of the substrate. For a silicon substrate, this impedance is approximately 75 Ω . The antenna design used in this work nominally yields a bandwidth of approximately 10 to 160 μm .

To maximize energy transfer to the detector element, its impedance must be matched to that of the antenna. This is the primary factor governing detector material selection, a conclusion arrived at in Ref. [5] in considering how to maximize detector responsivity \mathfrak{R} . This is defined for a current-biased device as the measured voltage output divided by the incident power on the detector. It is found that all metals are roughly equivalent as far as the optimization of \mathfrak{R} is concerned. Material selection is then governed by the requirement that the thin metallic film have a sheet resistance comparable to Z_a . Bulk niobium has a resistivity of $14.5 \mu\Omega \text{ cm}$ [9], which would nominally require 2-nm-thick films to obtain 75 Ω/square . This resistivity is not nearly as high as that of bismuth, $116 \mu\Omega \text{ cm}$, but we have found that using niobium films 20–30 nm thick causes the measured resistivity to be as much as twice the bulk value. This allows a well-matched detector to be constructed with a reasonable geometric aspect ratio.

The devices were fabricated on silicon substrates on which 250-nm-thick SiO_2 layers had been thermally grown. The oxide layer prevents the formation of Schottky barriers and increases the thermal isolation of the bolometer. The bolometer was formed of either a 20- or 30-nm nominal thickness niobium film, which was deposited using DC magnetron sputtering. The bolometer pattern was defined by RF plasma etching. The antenna is formed from 200-nm-thick gold which is evaporated by means of an electron beam and is patterned with a lift-off process.

The fabrication is a two-step, *ex-situ* process, so a cleaning step is required prior to the gold deposition to remove the oxide film which grows on the niobium upon exposure to air or water. This step was found to be the most critical part of the fabrication. The wafer is sputter-cleaned by admitting argon into the chamber at a pressure of 1.33 Pa (1×10^{-2} Torr), and igniting an RF plasma which develops a 400-V bias. The effectiveness of the cleaning step is sensitive to the base pressure to which the system is pumped prior to beginning the argon flow (performance was improved when lower base pressures were attained). Poorly cleaned detectors exhibited anomalous behavior in the dV/dI versus bias curve and a significant increase in voltage noise in the vicinity of 3 mA, making the devices usable only to about 2-mA bias.

The cleaning step was optimized by evaporating 100 nm of titanium with the wafer loaded in the chamber, but protected by a shutter.¹ The titanium acted as a getter to remove any residual gases present in the

¹When the gettering was performed, cleaning times in excess of 15 minutes resulted in removal of the niobium film in addition to the oxide. It was also observed that a second deposition system, in which no titanium was present, resulted in poorly cleaned detectors, even though it attained base pressures lower than 5×10^{-5} Pa. This appears to indicate that the process optimization may differ from system to system.

system. The sputter-cleaning was performed after the base pressure had been reduced to less than 5×10^{-5} Pa (3.5×10^{-7} Torr) by this procedure. A second evaporation of titanium was performed after the sputter-cleaning had been completed.

The sheet resistance of the niobium film was measured by including a 100- μm square test structure on each chip which was probed using the procedure outlined later for the bolometer resistance measurement. Measurements on 20-nm-thick niobium films indicate a value of $16 \pm 2.5 \Omega/\text{square}$, and for 30 nm the value measured is $12.5 \pm 1.2 \Omega/\text{square}$, where the errors are standard deviations obtained from measurements of 12 or more devices. In the case of the 20-nm film, this is twice the bulk value. The detector element is nominally $2.0 \times 0.8 \mu\text{m}$. However, comparison of the film resistivity to the bolometer resistance indicates that the effective number of squares (aspect ratio) for the detector is approximately 3–4.

Possible explanations for the high sheet resistance include reduction of the detector thickness by oxide growth, increased resistivity due to scattering of electrons from the film surfaces and from grain boundaries [10], and contact resistance between films. The larger than expected value of the effective number of squares may be due to small misalignments between films, or because there is a finite characteristic length at the feed over which current transfers between the films.

The effect of the higher niobium sheet resistance and higher effective aspect ratio is that detectors fabricated from 20–30 nm thick niobium films may be impedance matched to planar antennas on substrates without resorting to aspect ratios of more than 2 or 3 squares. We have been able to deposit films with repeatable results at these thicknesses. Bolometers fabricated from 20-nm-thick films had zero-bias resistances of $61 \pm 9 \Omega$, while those fabricated from 30-nm-thick films measured $39 \pm 5 \Omega$. Each of these provides an adequate match with reasonable reproducibility.

III. ELECTRICAL MEASUREMENTS

The responsivity $\mathfrak{R} = \beta I_{\text{bias}}$, where $\beta = \frac{1}{G} \frac{dR}{dT}$, was experimentally determined by measuring the small-signal differential resistance dV/dI as a function of the DC bias current and curve-fitting to obtain the responsivity coefficient β . The measurement was done using a four-wire resistance bridge operating at 16 Hz and 3- μA RMS. An adjustable DC current was superimposed on this to allow various biases. Contact was made to the chips by means of a wafer probe station.

The small-signal differential resistance is obtained from the expression relating the resistance of a bolometer with the power dissipated in it [5]

$$R = R_0 + \beta P \quad (2)$$

where R_0 is the zero-bias detector resistance. We assume that β is constant over the range of measurement, i.e., that the thermal conductance G is independent of temperature, that $R(T)$ is linear, and that at a fixed temperature the device is ohmic. Defining R as V/I and P as IV and rearranging terms an expression for the voltage across the bolometer is obtained

$$V = \frac{R_0 I}{1 - \beta I^2}. \quad (3)$$

This can be differentiated to give the expression for differential resistance

$$\frac{dV}{dI} = \frac{R_0(1 + \beta I^2)}{(1 - \beta I^2)^2}. \quad (4)$$

Because $\frac{dR}{dT} > 0$ a limit is imposed on bias current by self-heating of the bolometer, which leads to thermal runaway when the denominator of (4) becomes zero. This occurs at $I_{\text{bias(max)}} = 1/\sqrt{\beta}$

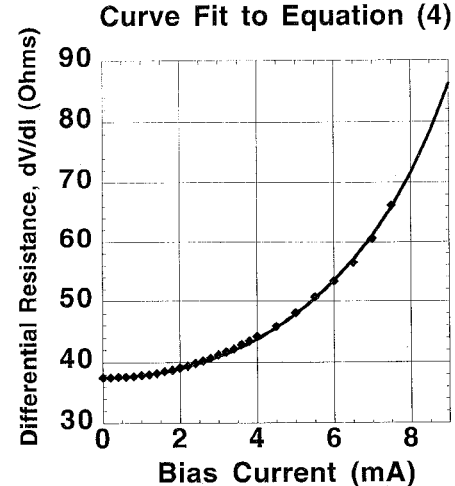


Fig. 1. A detector measured to 7.5 mA is fitted to (4). The extension of the curve fit beyond the measured data is calculated from the fitted responsivity coefficient β , which was $3.21 \text{ V}/(\text{W mA})$.

which limits the responsivity to $\mathfrak{R}_{\text{max}} = \sqrt{\beta}$. By applying a bias only long enough to stabilize the resistance bridge reading, we were able to bias a detector as high as 7.5 mA. This represents 44% of the $I_{\text{bias(max)}} = 17 \text{ mA}$ obtained from the fitted value $\beta = 3.4 \text{ V}/(\text{W mA})$ for this detector. The maximum stable bias achieved without initiating thermal runaway was 6.4 mA.

The ultimate figure of merit for a detector is its noise equivalent power (NEP), the input power necessary to give a signal-to-noise ratio of 1 per unit bandwidth. It is obtained experimentally by measuring the noise spectrum S_v of the detector and dividing by the responsivity

$$\text{NEP} = \frac{S_v}{\mathfrak{R}}. \quad (5)$$

Noise measurements were done by applying an adjustable DC bias from a 67-V battery in series with a resistance of 15–110 $\text{K}\Omega$. The noise voltage across the device was connected to the input of a low-noise amplifier (LNA) with a voltage gain of 100. The output signal was amplified again and then displayed on a spectrum analyzer. In addition to using shielded boxes for all components, we did the measurement in a shielded room to minimize interference from power line harmonics. The raw noise spectrum as measured in this setup includes several uncorrelated noise sources

$$S_v^2 = S_v^2(\text{Johnson}) + S_v^2(1/f) + S_v^2(\text{phonon}) + S_v^2(\text{amplifier}). \quad (6)$$

The noise components are given by

$$S_v^2(\text{Johnson}) = 4KTR, \quad (7)$$

$$S_v^2(1/f) \propto I^2 R^2 \frac{1}{f^n}, \quad (8)$$

$$S_v^2(\text{phonon}) = 4KT^2 G. \quad (9)$$

where (8) is an empirical relation [11] and $n \cong 1$.

The measured data was corrected for the $1.2 \text{ nV}/\sqrt{\text{Hz}}$ input noise of the first amplifier. This lowered the effective measurement floor to approximately $0.5 \text{ nV}/\sqrt{\text{Hz}}$. This measurement setup was verified by measuring the noise of several wirewound resistors. For resistance values of 48–200 Ω , the measured noise spectrum was flat and within 5% of the theoretical Johnson noise given by (7).

The measured voltage noise spectral densities of niobium detectors from two different wafers are shown in Fig. 2, together with data on a bismuth device from [5]. The $1/f$ noise was quantified by subtracting the calculated Johnson noise from Fig. 2 and curve-fitting to $S_v(1/f)$

Noise Spectra of Detectors

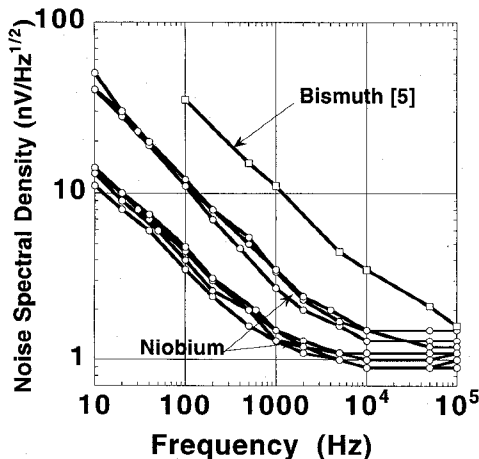


Fig. 2. The measured noise spectra of several detectors are shown at a bias of 3.6 mA. A noise spectrum of a bismuth detector from [5] is shown for comparison.

from (8) over the range of 10–5 kHz. The values obtained indicated that the $1/f$ noise is given approximately by

$$S_v(\text{nV}/\sqrt{\text{Hz}}) = m_1 \frac{I(\text{mA})}{(f(\text{kHz}))^{m_2}}, \quad (10)$$

where $I(\text{mA})$ is the DC bias current in mA, $f(\text{kHz})$ is the frequency in kHz, and m_1 and m_2 are fitted parameters. The parameter m_1 had a median value of 0.39 and the parameter m_2 had a median value of 0.53. The curves in Fig. 2 indicate that the niobium devices have $1/f$ noise spectra approximately a factor of 7 lower than bismuth devices. This improvement in noise, and not an increase in responsivity, is the reason that lower NEP's are obtained for the niobium detectors than for bismuth detectors with equivalent thermal isolation. Indeed, NEP's are obtained from these niobium detectors which are roughly equivalent to those of bismuth devices fabricated on free-standing airbridges to improve thermal isolation. Niobium airbridges could be built, though a buffer layer would be required to define a structurally sound airbridge using such thin films.

As the bias is applied, the $1/f$ component becomes apparent (initially, only Johnson noise is seen) and increases with bias so that the “corner” frequency, at which the noise is a factor of 2 larger than in the Johnson noise-limited region, shifts upward with bias. This makes the optimum bias, that at which the NEP is a minimum, frequency dependent. We have chosen 3.6 mA bias for our figures and tables. At this bias the $1/f$ corner is approximately 1 kHz, below which the devices are limited by $1/f$ noise, while above 10 kHz they are limited by Johnson noise. The physical explanation for the lower $1/f$ noise we observe in Nb bolometers compared to previous Bi devices is very much an open question, as is the much more general issue of $1/f$ noise in metal films [11].

It is possible to extract a value for the thermal conductance G from the curve fits performed to determine responsivity, if dR/dT is assumed to be equal to R_0/T_0 . Calculated values of this parameter and of the Johnson-limited and phononlimited noise equivalent powers of the detectors plotted in the figures are summarized in Table I.

IV. CONCLUSION

Antenna-coupled microbolometers using niobium as the detector element are readily constructed monolithically without any exotic steps taken to increase thermal isolation. They have extremely low $1/f$ noise, which is a property of the material used and which is

TABLE I
THE CALCULATED THERMAL CONDUCTANCE AND JOHNSON-LIMITED AND PHONON-LIMITED NEP OF SIX DETECTORS IS SHOWN. THE FIRST THREE COLUMNS ARE THE MEASURED BOLOMETER RESISTANCE AT DC BIAS CURRENTS OF 0 AND 3.6 mA (R_0 AND $R_{3.6}$), AND THE RESPONSIVITY AT 3.6 mA ($R_{3.6}$). THE REMAINING COLUMNS ARE CALCULATED FROM THESE MEASUREMENTS AND ARE THE DETECTOR TEMPERATURE AT 3.6 mA ($T_{3.6}$), THE THERMAL CONDUCTANCE OF THE DETECTOR (G), AND THE JOHNSON AND PHONON NOISE EQUIVALENT POWER AT 3.6 mA (NEP_J AND NEP_P)

R_0 (Ω)	$R_{3.6}$ mA (Ω)	$R_{3.6}$ mA (V/W)	$T_{3.6}$ mA (K)	G (W/K)	NEP _J (W/ $\sqrt{\text{Hz}}$)	NEP _P (W/ $\sqrt{\text{Hz}}$)
58.0	67.6	13.9	349	5.0×10^{-5}	8.2×10^{-11}	1.3×10^{-12}
34.8	39.4	11.5	340	3.6×10^{-5}	7.5×10^{-11}	1.3×10^{-12}
44.7	53.0	15.1	356	3.6×10^{-5}	6.8×10^{-11}	1.0×10^{-12}
35.2	40.1	9.9	342	3.6×10^{-5}	8.8×10^{-11}	1.5×10^{-12}
40.6	47.5	14.4	351	3.4×10^{-5}	6.6×10^{-11}	1.0×10^{-12}
37.5	42.9	12.3	343	3.7×10^{-5}	7.3×10^{-11}	1.3×10^{-12}

Technology Comparison

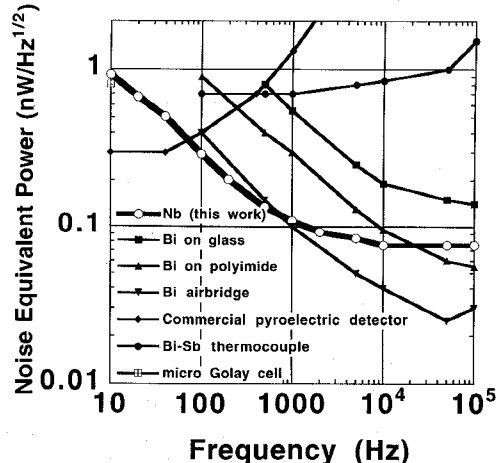


Fig. 3. The NEP of our best detector is compared to figures obtained from [1], [5], [6], and [12].

approximately given in $\text{nV}/\sqrt{\text{Hz}}$ by $0.39 \frac{I(\text{mA})}{\sqrt{f(\text{kHz})}}$, approximately a factor of 7 lower than bismuth microbolometers. A comparison of the NEP obtained from these detectors with that of some other infrared detectors in Fig. 3 indicates that these detectors offer dramatically improved noise performance. There is the possibility of lowering the NEP further by taking additional measures to thermally isolate the detector, thereby improving the responsivity. The NEP's we have obtained are comparable to bismuth airbridges, approximately a factor of 5 better than bismuth detectors on glass, and better than detectors which exhibit no $1/f$ noise (pyroelectrics and thermocouples) at all but the lowest frequencies.

ACKNOWLEDGMENT

We are grateful to Professor Zoya Popovic at the University of Colorado at Boulder for extensive advice and discussions.

REFERENCES

- [1] T. W. Kenney, W. J. Kaiser, S. B. Waltman, and J. K. Reynolds, "Novel infrared detector based on a tunneling displacement transducer," *Appl. Phys. Lett.*, vol. 59, no. 15, pp. 1820-1822, Oct. 7, 1991.
- [2] C. C. Ling and G. M. Rebeiz, "A wide-band monolithic quasioptical power meter for millimeter- and submillimeter-wave applications," *IEEE Trans. Microwave Theory Tech.*, vol. 39, no. 8, pp. 1257-1261, Aug. 1991.
- [3] T. -L. Hwang, S. E. Schwarz and D. B. Rutledge, "Microbolometers for infrared detection," *Appl. Phys. Lett.*, vol. 34, no. 11, pp. 773-776, June 1, 1979.
- [4] D. B. Rutledge, D. P. Neikirk, and D. P. Kasingam, "Integrated circuit antennas," in *Infrared and Millimeter Waves*, vol. 10, K. J. Button, Ed. New York: Academic, 1983.
- [5] D. P. Neikirk, W. W. Lam, and D. B. Rutledge, "Far-infrared microbolometer detectors," *Int. J. Infrared and Millimeter Waves*, vol. 5, no. 3, pp. 245-278, 1984.
- [6] D. P. Neikirk and D. B. Rutledge, "Self-heated thermocouples for far-infrared detection," *Appl. Phys. Lett.*, vol. 41, no. 5, pp. 400-402, Sept. 1982.
- [7] D. P. Neikirk and D. B. Rutledge, "Air-bridge microbolometer for far-infrared detection," *Appl. Phys. Lett.*, vol. 44, no. 2, pp. 153-155, Jan. 15, 1984.
- [8] E. N. Grossman, J. E. Sauvageau and D. G. McDonald, "Lithographic spiral antennas at short wavelengths," *Appl. Phys. Lett.*, vol. 59, no. 25, pp. 3225-3227, Dec. 16, 1991.
- [9] C. Kittel, *Introduction to Solid State Physics*, 6th ed. New York: Wiley, 1986.
- [10] T. J. Coutts, *Electrical Conduction in Thin Metal Films*. Amsterdam: Elsevier Scientific, 1974.
- [11] P. Dutta and P. M. Horn, "Low-frequency fluctuations in solids: 1/f noise," *Rev. Mod. Phys.*, vol. 53, no. 3, pp. 497-516, July 1981.
- [12] P1-70 Ultra-Low Noise Pyroelectric Detector/FET Preamp. Molelectron Detecto, Inc., Portland OR, 1990.

A Planar Quasi-Optical Mixer Using a Folded-Slot Antenna

Stephen V. Robertson, Linda P. B. Katehi, and Gabriel M. Rebeiz

Abstract—A quasi-optical mixer using only planar structures such as coplanar-waveguide and slotline is presented. The mixer, which can be scaled for millimeter-wave applications and placed on a substrate lens, uses orthogonal modes in a folded-slot antenna to achieve intrinsic RF/LO isolation without RF filtering or subharmonic pumping. The folded-slot balanced mixer was fabricated on RT/Duriod and obtained a minimum isotropic conversion loss of 1.2 dB at 11.6 GHz. Numerical integration of full two-dimensional antenna patterns yielded an antenna directivity of 7 dB, corresponding to a single side-band (SSB) mixer conversion loss of 8.2 dB. The mixer demonstrated -18 dB RF/IF isolation and -30 dB LO/IF isolation.

I. INTRODUCTION

Planar circuit designs are advantageous for producing millimeter-wave integrated circuits because they can be easily fabricated using monolithic techniques. Uniplanar circuit structures such as coplanar-waveguide (CPW) and slotline are especially useful since they

Manuscript received March 21, 1994; revised August 5, 1994. This work was supported by Texas Instruments, Inc.

The authors are with the Department of Electrical Engineering and Computer Science, The University of Michigan, Ann Arbor, MI 48109-2122 USA.

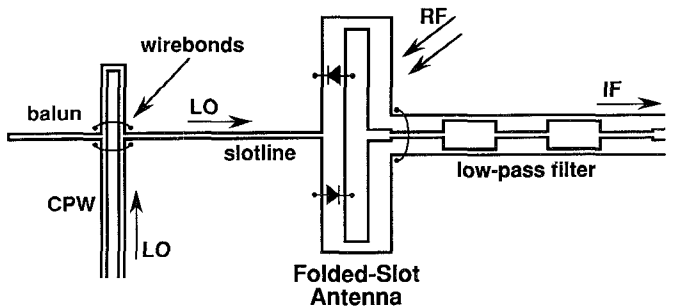


Fig. 1. Layout of the folded-slot balanced mixer circuit (reprinted from the 23rd *Euro. Microwave Conf. Dig.*).

eliminate the need for via holes or backside metallization and can be integrated with solid-state devices on a single surface [1]. In the past, planar microwave and millimeter-wave receivers have employed quasioptical techniques to achieve compact size and reduced transmission line loss [2]–[4]. Also, planar quasioptical receivers have exploited symmetry to realize balanced mixers [5].

This paper explores the realization of a quasi-optical mixer with uniplanar structures. First, the folded-slot antenna is investigated as a planar quasi-optical mixing element. Then, slotline and CPW structures are used to implement the LO pumping network and the low-pass IF filter. In the circuit configuration of Fig. 1, diodes are mounted in the slots of the antenna to provide mixing between the received RF and injected LO signals. The mixer achieves balanced mixing with good conversion loss and high port-to-port isolation.

II. FOLDED-SLOT ANTENNA

The development of the folded-slot antenna was based on previously published work on coplanar-waveguide antennas [4]–[7] and was first proposed as a microshield line antenna by Rexberg *et al.* [8]. Two main characteristics of the folded-slot antenna make it especially useful for a quasioptical mixing application: 1) a planar geometry, and 2) the ability to support two orthogonal resonant modes.

Theoretical analysis of the antenna based on an SDIE method [9] shows that the folded-slot antenna is at first resonance when the length of the slots is approximately equal to half of the guided wavelength. This resonance can exist for both a CPW feed, which excites an even mode, and a slotline feed, which excites an odd mode. Fig. 2 depicts the field distributions of both of these modes for a folded-slot antenna in the first resonance. In the even mode (CPW feed) the field distribution in the slots is similar to the current distribution on a folded dipole, and the slots radiate in phase. In the odd mode (slotline feed) the slots are excited with a 180° phase difference, and therefore do not radiate. It is possible to excite both odd and even modes simultaneously by feeding the antenna from opposite sides with a CPW and a slotline. In this case, the two modes will not couple to each other since they are orthogonal. Feeding the antenna on adjacent sides with similar feed lines (either both CPW or both slotline) achieves the same result. Alternatively, similar feeds on opposite sides of the antenna will couple to the same mode with a 180° phase difference at the two feed points. In this work, the folded-slot mixer receives the RF quasi-optically in the even mode, and a slotline excites the LO in the odd mode. Thus intrinsic isolation between the two orthogonal modes serves the purpose of RF/LO isolation.